

Improvement in the Design Calculations of Multi-Ring Permanent Magnet Thrust Bearing

Siddappa I. Bekinal^{1, *} and Mrityunjay Doddamani²

Abstract—This article presents the design and optimization of multi-ring permanent magnet thrust bearing (PMTB) with an axial air gap between successive axial stacks. Larger air gap due to the inclusion of conductive materials needs to be critically analysed in permanent magnet bearings with eddy current damper. High conductivity materials can be filled in an axial air gap instead of a radial air gap to increase the required amount of damping. Three-dimensional (3D) mathematical model for load-carrying capacity for the said configuration is presented using the Coulombain model. The significance of an axial air gap between successive ring pairs in the configuration concerning maximization in the bearing characteristics is presented. Variables such as the number of axial stacks, an axial air gap between the successive rings, an inside radius of rotor ring magnets, and an inside radius of stator ring magnets are optimized at different air gap values for maximizing the load-carrying capacity and stiffness. A significant increase in the values of bearing characteristics is observed in the optimized configuration as compared to bearing with a single permanent magnet ring pair. Optimized PMTB with comparable load carrying capacity and stiffness values can be used to replace conventional bearings used in high-speed applications to improve system efficiency.

1. INTRODUCTION

Permanent magnet bearings (PMBs) [1–3] are friction and lubrication-free bearings having lower maintenance as compared to conventional bearings. These are simpler due to the absence of sensors, actuators, and electronic equipment required in the effective functioning of active magnetic bearings [4]. In high-speed applications [5–8] where the aforementioned features are highly desirable, PMB is the most suitable candidate to enhance the system efficiency. The load-carrying capacity and stiffness of PMB consisting of only one ring pair can be determined using two-dimensional (2D) [9–12] or 3D [13–18] equations and these features are too low as compared to the conventional bearings. Yonnet et al. [19] introduced the concept of stacked structures with significant enhancement in the stiffness value. Further, many researchers [20–22] presented the equations to address the calculation of bearing features in multi-ring PMB. Optimization of geometrical dimensions of PMB for achieving their maximum characteristics was presented by the number of researchers in radial [23, 24] and thrust [25–30] bearings. In the preceding literature on optimization of PMB, researchers focussed on the following points; (i) multi-layer radial PMB was optimized in a given cylindrical volume for maximum radial stiffness using finite element simulation method [23], whereas complete optimization was carried out in [24] using 3D equations for maximizing radial force. Also, generalized equations were provided for mean radius and clearance in given axial length and outer radius of the stator, (ii) different multi-layer thrust PMB structures were optimized for maximum bearing characteristics using 2D [25, 26] as well as 3D [27, 28]

Received 24 May 2020, Accepted 1 July 2020, Scheduled 11 July 2020

* Corresponding author: Siddappa Iranna Bekinal (siddappabekinal@gmail.com).

¹ Department of Mechanical and Manufacturing Engineering, Manipal Institute of Technology, Manipal Academy of Higher Education, Manipal, Udipi, Karnataka 576104, India. ² Department of Mechanical Engineering, National Institute of Technology Karnataka, Surathkal, Mangalore, Karnataka 575025, India.

equations and the process of optimization was for a control volume, (iii) Lijesh et al. [29] presented multi-objective optimization of radial PMB for maximum force and stiffness in a given volume and generalized equations for optimized parameters of multi-layer PMB in terms of a single layer. Despite significant contribution towards the enhancement in PMB characteristics with the aid of optimization, low damping is the major issue. Although, damping can be increased by active [30] or passive [31] means, later one is simple and can be achieved by including conductive material in the magnetic space. The inclusion of conductive materials between stator and rotor magnets creates a larger air gap and thereby decreases the force and stiffness of PMB. The conductive material can be included by providing an axial air gap between successive ring pairs to achieve larger stiffness and the required amount of damping. Yoo et al. [32] demonstrated the presence of optimal axial air gap between axially polarized successive ring magnets for maximum axial force and optimized the stacked structures for the required load-carrying capacity using 2D equations. Optimization of standard and Halbach structures with air or iron intervals for achieving maximum stiffness per magnet volume ratio was presented in [33] using 2D equations. Besides, the authors mentioned that the stiffness of the Halbach structure does not improve by providing air intervals. This paper presents a 3D mathematical model for a load-carrying capacity generated in axially polarized multi-ring PMTB with an axial air gap between successive rings which is not addressed in the earlier research efforts. Further, the axial air gap is optimized for an optimized number of axial stacks (n_{opt}) for a given axial length of bearing. Finally, bearing geometrical dimensions ($R1$ and $R3$) are optimized by taking into the account of n_{opt} and an optimum axial air gap (ag_{opt}) for different values of the air gap.

2. PERMANENT MAGNET BEARING GEOMETRIES

Single ring pair PMTB with stator and rotor rings is shown in Fig. 1(a), and its geometrical dimensions are listed in Table 1. This bearing geometry having a low force and stiffness can be replaced by multi-ring PMTB (refer Fig. 1(b)) in the same axial length ' L ' to enhance the force and stiffness. The same multi-ring PMTB with an axial air gap (ag) between adjacent axial stacks is represented in Fig. 1(c).

Table 1. Geometrical dimensions of single ring pair PMTB.

Parameter	Value
Inside radius of the rotor ring magnet, $R1$ (mm)	10
Outside radius of the rotor ring magnet, $R2$ (mm)	20
Inside radius of the stator ring magnet, $R3$ (mm)	22
Outside radius of the stator ring magnet, $R4$ (mm)	32
Air gap thickness, g (mm)	2
Axial length, L (mm)	30
Magnetic polarization, B_r (T)	1.2

3. MATHEMATICAL MODEL

The generalized mathematical equation for load-carrying capacity in axially magnetized multi-ring PMTB structure with an axial air gap is presented in this section. In the selected bearing structure, rings were stacked one adjacent to another with an air gap in the axial direction. Interaction between the u th ring of a rotor and the v th ring of a stator in multi-ring PMTB is shown in Fig. 2.

The equation for load-carrying capacity in multi-ring PMTB with an axial air gap between successive rings is expressed as,

$$F_Z = \frac{B_r^2}{4\pi\mu_0} \sum_{u=1}^n \sum_{v=1}^n \sum_{k=1}^2 \sum_{l=3}^4 \sum_{p=1}^m \sum_{q=1}^m \frac{S_{pku} S_{qlv}}{R_{(pku)(qlv)}^3} \mathbf{R}_{(pku)(qlv)} (-1)^{(k+l)} (-1)^{(u+v)} \quad (1)$$

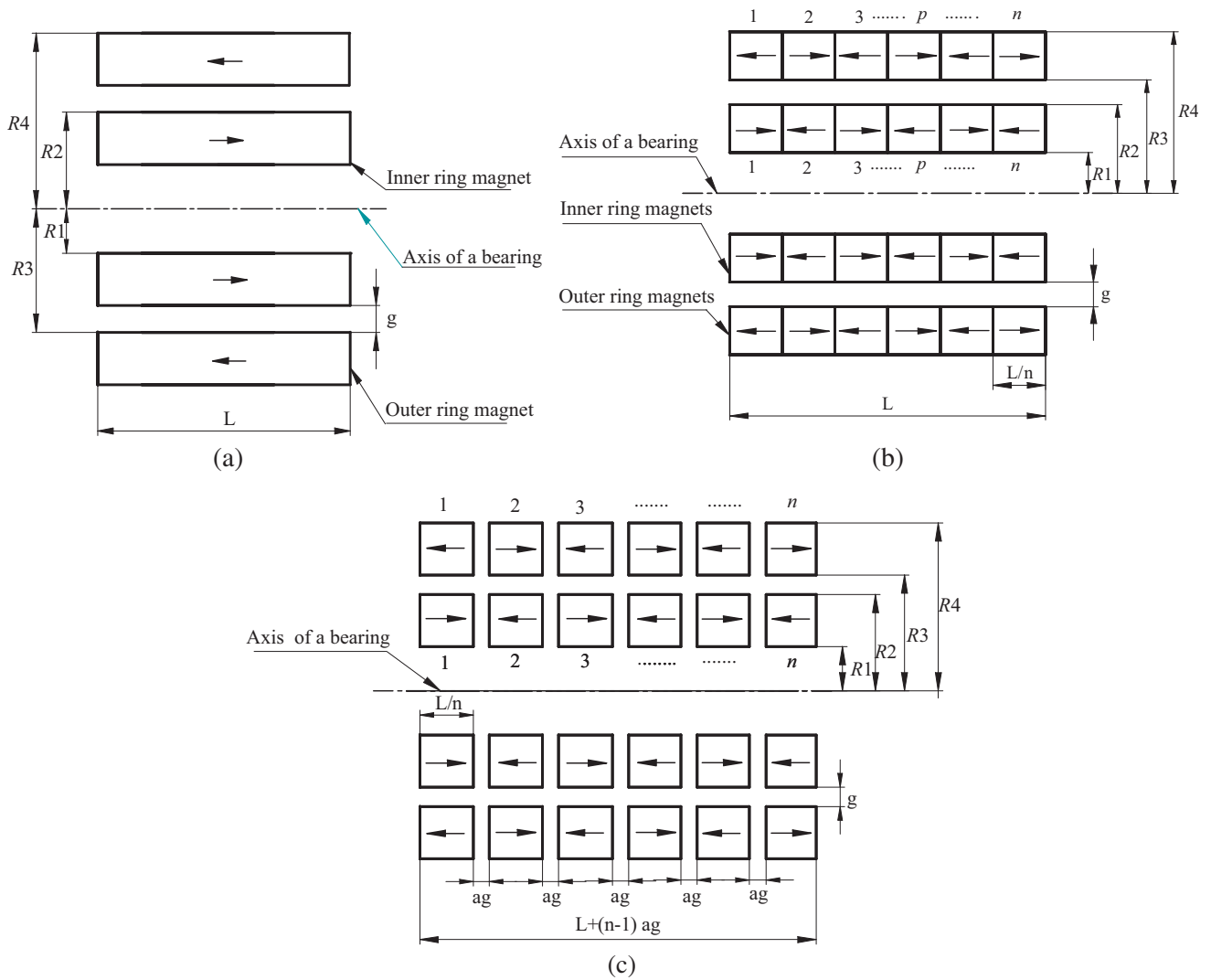


Figure 1. PMTB structures with (a) single ring pair, (b) multi-ring pairs and (c) axial air gap between successive axial stacks.

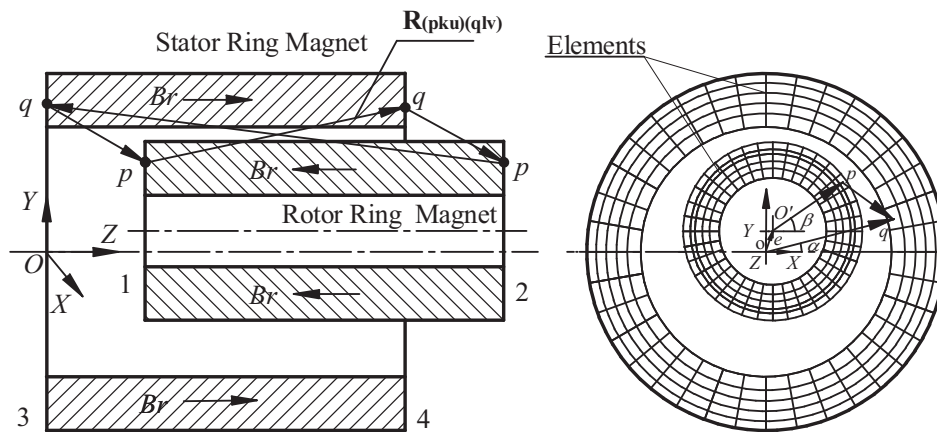


Figure 2. Magnetic interaction between two rings in multi-ring PMTB.

where $\mathbf{R}_{(\mathbf{pku})(\mathbf{qlv})} = (X_{qlv} - X_{pku})\mathbf{i} + (Y_{qlv} - Y_{pku})\mathbf{j} + (Z_{qlv} - Z_{pku})\mathbf{k}$ is the position vector, and coordinates of elements on the faces of magnets are,

$$\begin{aligned} (X_{pku})_{1,2} &= (x + r_{mr} \cos \beta) \mathbf{i} & (X_{qlv})_{3,4} &= (r_{ms} \cos \alpha) \mathbf{i} \\ (Y_{pku})_{1,2} &= (y + r_{mr} \sin \beta) \mathbf{j} & (Y_{qlv})_{3,4} &= (r_{ms} \sin \alpha) \mathbf{j} \\ (Z_{pku})_1 &= (z + (u - 1)l + (u - 1)ag) \mathbf{k} & (Z_{qlv})_3 &= ((v - 1)l + (v - 1)ag) \mathbf{k} \\ (Z_{pku})_2 &= (z + (u)l + (u - 1)ag) \mathbf{k} & (Z_{qlv})_4 &= (vl + (v - 1)ag) \mathbf{k} \end{aligned} \quad (2)$$

Suffix 1, 3 and 2, 4 are the left and right surfaces of rotor and stator, respectively. The complete description of all parameters can be referred from [27].

The axial stiffness of the proposed PMTB structure is given by,

$$K_z = \frac{dF_z}{dZ} = \frac{1}{2\Delta Z} [F_z(Z + \Delta Z) - F_z(Z - \Delta Z)] \quad (3)$$

4. SIGNIFICANCE OF AN AXIAL AIR GAP

In this section, an optimized configuration (refer Table 2) without an axial air gap between successive rings presented in our earlier research work [27] is selected and analysed for an axial load and stiffness with an axial air gap using the proposed mathematical model. The optimized value of an axial air gap is calculated by varying its value for maximum bearing features and results are plotted in Fig. 3. The axial load of the configuration (462.69 N at $ag_{opt} = 2$ mm) and stiffness (321089.14 N/m at $ag_{opt} = 0.6$ mm) increases by 19% and 3.2% respectively as compared to a structure without an axial air gap.

Table 2. Geometrical dimensions of an optimized configuration [27].

Parameters	Optimized parameters for maximum load-carrying capacity, $F_{z \max} = 389.38$ N	Optimized parameters for maximum axial stiffness, $K_{z \max} = 311214.1$ N/m
z (m)	0.0025	0
n	4	6
$R1$ (m)	0.004	0.0085
$R2$ (m)	0.015	0.0155
$R3$ (m)	0.016	0.0165
$R4$ (m)	0.02	0.02

5. OPTIMIZATION AND RESULTS

The mathematical Equations (1)–(3) presented in the previous section are solved in MATLAB for load-carrying capacity and stiffness in a single (Fig. 1(a)) and multi-ring pair PMTB without (Fig. 1(b)) and with (Fig. 1(c)) an axial air gap between successive ring pairs. The calculated value of load-carrying capacity (259.89 N) and stiffness (59630 N/m) of a bearing structure shown in Fig. 1(a) and for the properties given in Table 1 are too low as compared to the conventional bearings. To replace conventional bearings by PMB, optimization of different parameters such as the number of axial stacks (n), axial air gap (ag) between the successive rings, inside radius of rotor ring magnets ($R1$) and inside radius of stator ring magnets ($R3$) for maximum load-carrying capacity and stiffness is necessary. Steps followed for an optimization process are given below,

1. Initially, load-carrying capacity and stiffness values are determined for single ring pair (Fig. 1(a)) with an axial length of 30 mm.

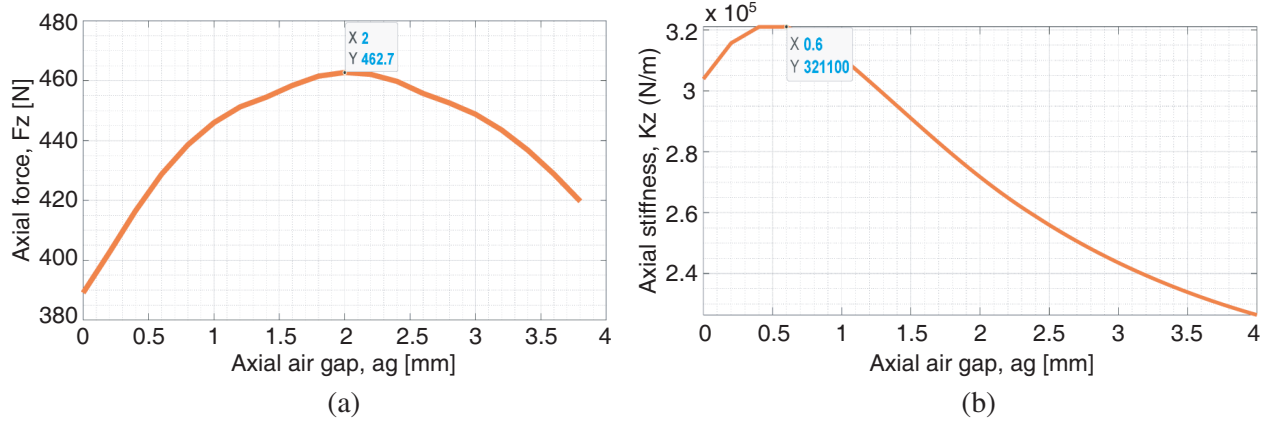
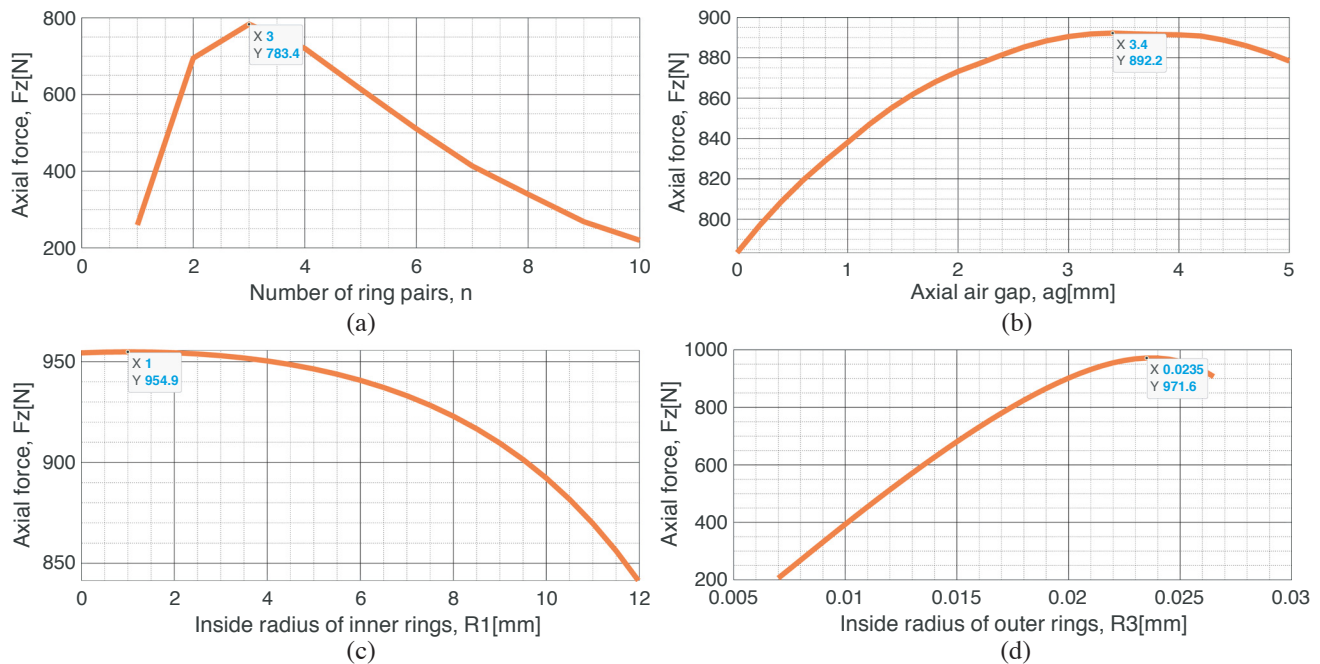


Figure 3. Characteristics of the bearing structure presented in [27] for the axial air gap. (a) Load-carrying capacity. (b) Axial stiffness.

2. The number of axial stacks ‘ n ’ is varied in the same axial length of 30 mm by taking into the account of an optimum value of the axial offset (which is $L/2$ for maximum load-carrying capacity and zero for maximum stiffness) to determine an optimum value, i.e., ‘ n_{opt} ’ for the same magnet volume.
3. Then, an axial air gap (ag) between successive rings is varied at ‘ n_{opt} ’ to calculate ‘ ag_{opt} ’.
4. Further, the inside radius of rotor rings ($R1$) is varied at ‘ n_{opt} ’ and ‘ ag_{opt} ’ to get ‘ $R1_{opt}$ ’.
5. Finally, the inside radius of stator rings ($R3$) is optimized at ‘ n_{opt} ’, ‘ ag_{opt} ’ and ‘ $R1_{opt}$ ’.

Initially, optimization is carried out for the selected structure (Fig. 1(a)) for an air gap of 2 mm by varying aforementioned parameters for maximum load-carrying capacity and stiffness and optimized results are shown in Figs. 4(a)–(d) and 5(a)–(d). Maximized values corresponding to different optimized parameters along with results of single ring pair PMTB are given in Fig. 4(e) and Fig. 5(e).

It is observed that the maximized value of load carrying capacity is 971.6 N (274% higher) and stiffness 377200 (533% higher) as compared to single ring pair bearing.



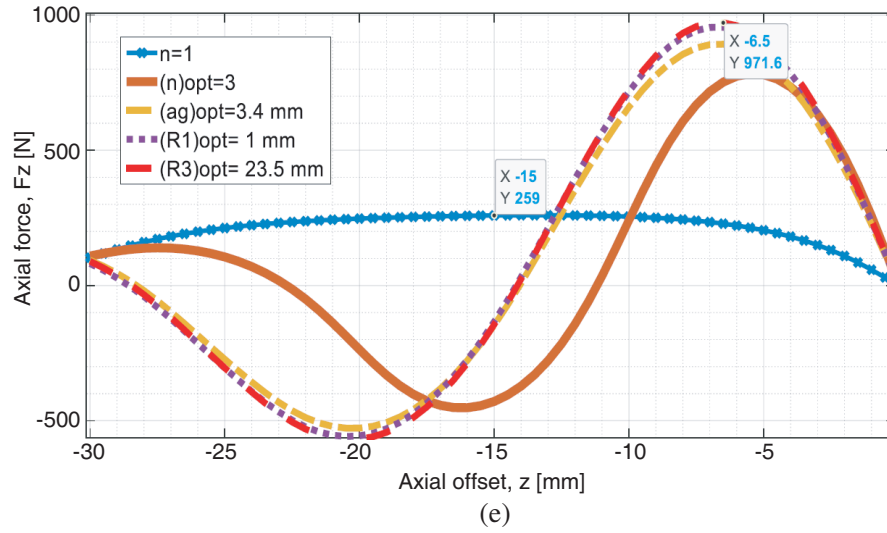
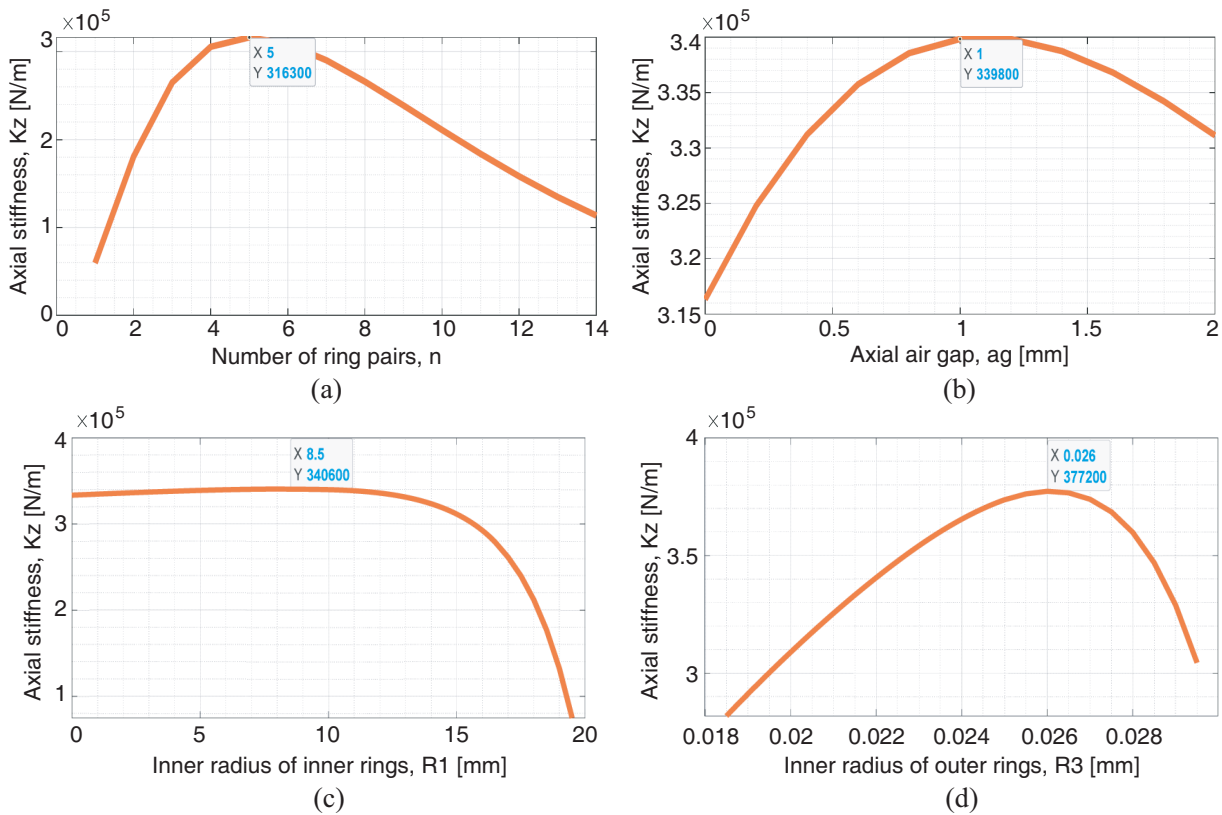


Figure 4. Optimized parameters for maximum load-carrying capacity. (a) Number of axial stacks. (b) Axial air gap. (c) Inside radius of rotor rings. (d) Inside radius of stator rings and (e) comparison of results.

Further, an optimization is extended for different air gap values ranging from 0.2 to 3 mm in steps of 0.2 mm. Variation of bearing characteristics with the number of axial stacks for different air gap values is shown in Fig. 6 and an optimum number of axial stacks with maximum bearing characteristics are given in Table 3. It is observed that the optimum number of axial stacks decreases with an increase in the air gap for maximum load-carrying capacity and stiffness values in an axial length of 30 mm.



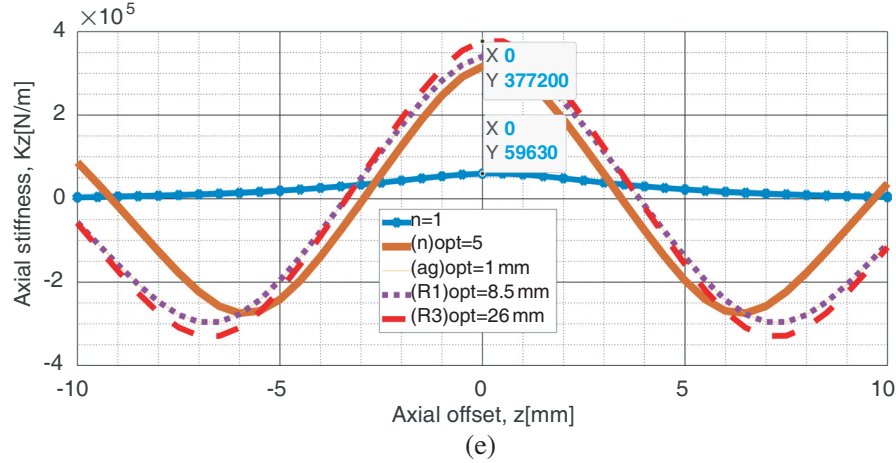


Figure 5. Optimized parameters for maximum axial stiffness. (a) Number of axial stacks. (b) Axial air gap. (c) Inside radius of rotor rings. (d) Inside radius of stator rings and (e) comparison of results.

Table 3. Optimum values of the number of axial stacks and axial air gap for maximum bearing characteristics.

Air gap, g (mm)	Load carrying capacity, F_z [N]				Axial stiffness, K_z [N/m]			
	n_{opt}	$F_{z\ max}$	ag_{opt} (mm)	$F_{z\ max}$ at ag_{opt}	n_{opt}	$K_{z\ max}$	ag_{opt} (mm)	$K_{z\ max}$ at ag_{opt}
0.2	5	1349.22	2.4	1576.17	12	1203528.68	0.4	1307562.29
0.4	5	1240.76	2.8	1474.28	11	976016.03	0.6	1068936.81
0.6	4	1156.93	2.8	1328.45	9	807384.87	0.6	865884.53
0.8	4	1082.96	2.8	1258.92	8	678966.63	0.6	726762.72
1.0	4	1013.01	3.2	1192.59	7	579439.61	0.6	616212.98
1.2	3	949.84	3.2	1047.04	7	503309.31	0.8	545986.34
1.4	3	905.61	3.2	1006.03	6	441726.81	0.8	472122.87
1.6	3	863.14	3.2	966.50	6	391400.22	1.0	425687.58
1.8	3	822.41	3.4	928.62	5	349917.06	1.0	371081.99
2.0	3	783.40	3.4	892.22	5	316327.74	1.0	339828.32
2.2	3	746.07	3.8	858.01	5	286366.48	1.2	312316.15
2.4	3	710.38	4.0	825.19	5	259560.76	1.2	287754.11
2.6	3	676.30	4.0	793.75	4	239446.52	1.2	253133.58
2.8	3	643.76	4.0	763.55	4	221292.69	1.4	236180.12
3.0	3	612.73	4.2	734.69	4	204718.73	1.4	220814.22

After knowing the optimized axial stacks, an axial air gap between successive ring pairs is varied for different air gaps for maximum load-carrying capacity and stiffness keeping the thickness of inner and outer rings constant and results are plotted in Fig. 7 and tabulated in Table 3. Results show that the optimum value of the axial air gap increases with an increase in the air gap for maximum load-carrying capacity and stiffness.

The inside radius of rotor rings of the bearing configuration is varied by keeping optimized axial stacks (n_{opt}) and optimum axial air gap (ag_{opt}) constant at different air gaps for maximum bearing characteristics, and results are shown in Fig. 8 and given in Table 4. The optimum value of $R1$

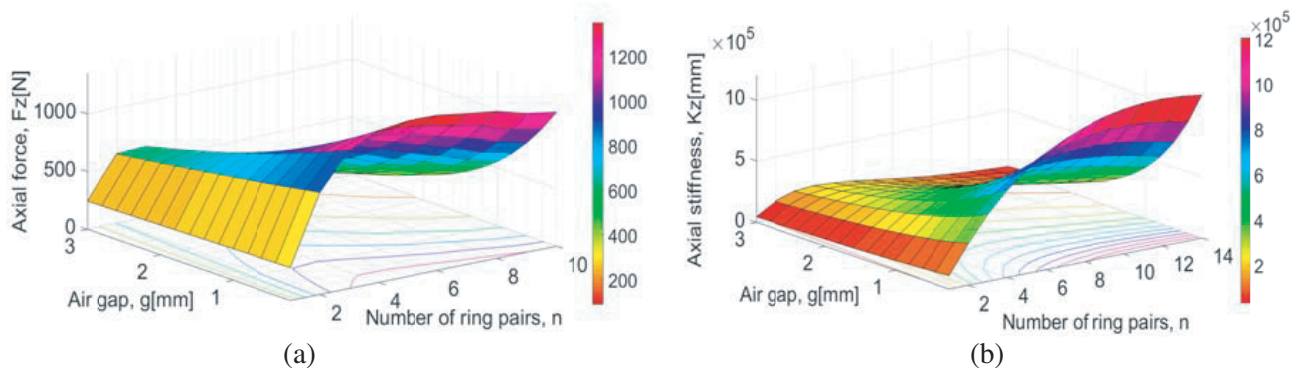


Figure 6. Variation of bearing characteristics with the number of ring pairs. (a) Load-carrying capacity. (b) Axial stiffness.

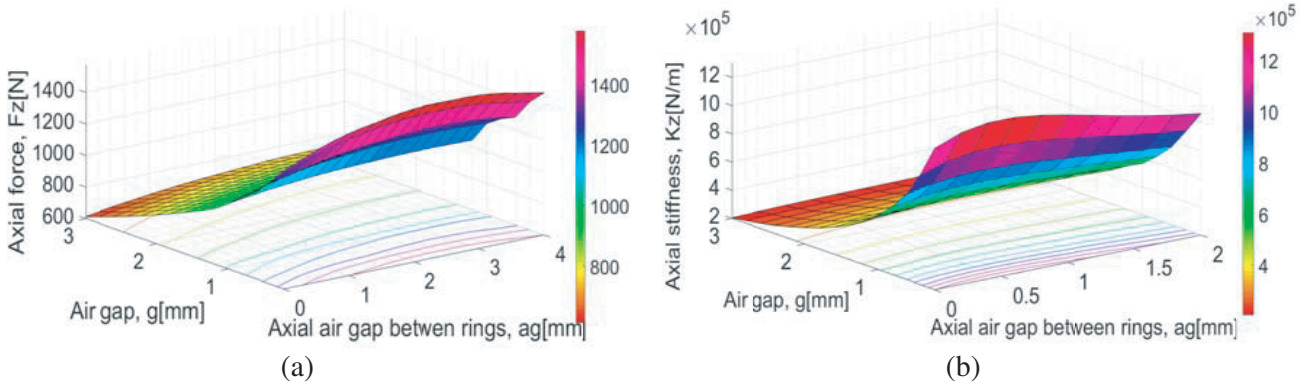


Figure 7. Variation of bearing characteristics with an axial air gap between ring pairs. (a) Load-carrying capacity. (b) Axial stiffness.

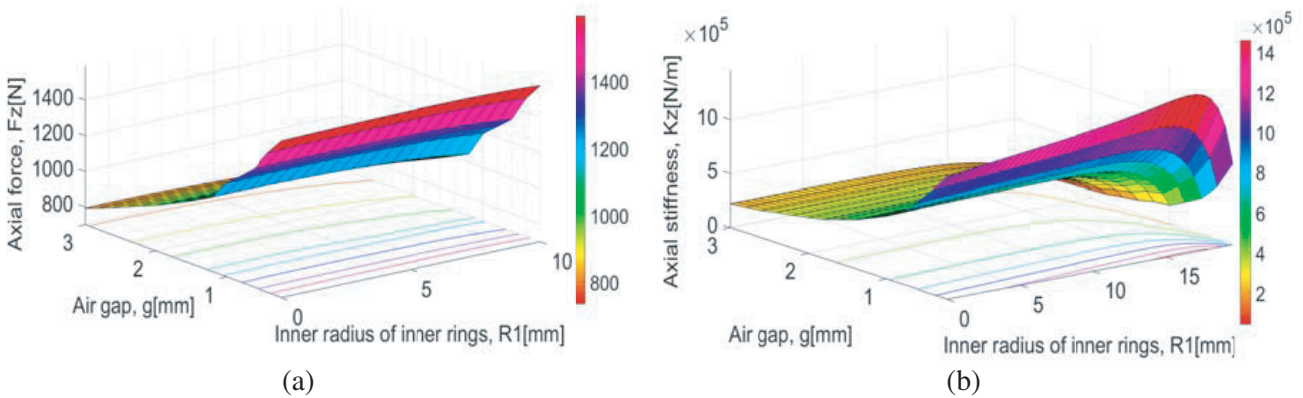


Figure 8. Variation of bearing characteristics with an inner radius of inner rings for different air gap values. (a) Load-carrying capacity. (b) Axial stiffness.

decreases with an increase in the air gap up to 1 mm, and it becomes constant with a further increase for maximum load-carrying capacity, whereas in the case of stiffness maximization, the optimum value decreases with an increase in the air gap.

The inside radius of stator rings (R_3) is varied at optimized values of n , ag , and R_1 for different air gaps for maximum values of bearing characteristics, and results are shown in Fig. 9. It is observed that the optimized value of R_3 is independent of an air gap, and its value is 24 mm and 26 mm for maximum load-carrying capacity and stiffness values, respectively.

Table 4. Optimum values of the inner radius of inner rings for maximum bearing characteristics at optimized values of (n) and (ag).

Air gap, g (mm)	Axial force, F_z [N]				Axial stiffness, K_z [N/m]			
	$R1_{opt}$ (mm)	n_{opt}	ag_{opt} (mm)	F_z max at ag_{opt} and n_{opt}	$R1_{opt}$ (mm)	n_{opt}	ag_{opt} (mm)	K_z max at ag_{opt} and n_{opt}
0.2	6	5	2.4	1592.85	16.5	12	0.4	1457178.70
0.4	5.5	5	2.8	1493.57	15.5	11	0.6	1125540.10
0.6	3	4	2.8	1368.38	14.5	9	0.6	886365.23
0.8	3	4	2.8	1296.91	13.5	8	0.6	735735.21
1.0	3	4	3.2	1229.44	12	7	0.6	613015.59
1.2	1	3	3.2	1118.26	11.5	7	0.8	547392.53
1.4	1	3	3.2	1074.59	10.5	6	0.8	472206.34
1.6	1	3	3.2	1032.53	10	6	1.0	425687.58
1.8	1	3	3.4	993.59	8.5	5	1.0	371785.37
2.0	1	3	3.4	954.85	8.5	5	1.0	340560.68
2.2	1	3	3.8	922.18	8	5	1.2	313323.84
2.4	1	3	4.0	888.42	7.5	5	1.2	289017.19
2.6	1	3	4.0	854.85	6	4	1.2	256514.02
2.8	1	3	4.0	822.59	5.5	4	1.4	239815.31
3.0	1	3	4.2	792.91	5	4	1.4	224325.31

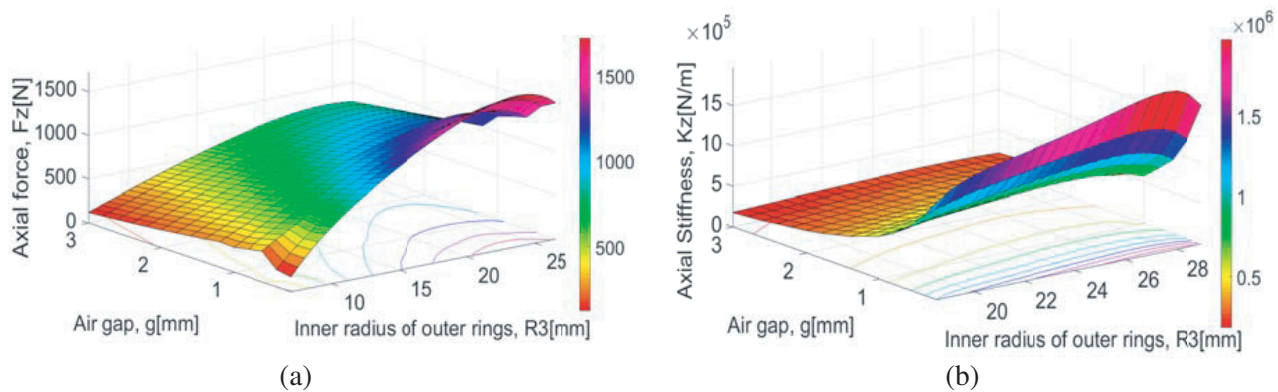


Figure 9. Variation of bearing characteristics with an inner radius of outer rings for different air gap values. (a) Load-carrying capacity. (b) Axial stiffness.

6. CONCLUSIONS

Multi-ring PMTB with an axial air gap between successive axial stacks is designed and optimized for maximum bearing features in a given axial length of the magnet. The optimized bearing configuration could be used to develop PMTB with an eddy current damper in which there is a scope for including conductive material in an axial air gap for maximum stiffness and damping coefficient.

The following conclusions are drawn based on this research work,

- Maximized values of load carrying capacity and stiffness increase by 3.73 and 6.32 times respectively in the selected geometry of bearing for an air gap of 2 mm.
- An optimum value of the axial air gap is a dependent parameter as its value increases with an air gap and increases with a decrease in the number of optimized axial stacks.
- The optimized value of $R1$ decreases with an increase in the air gap whereas $R3$ is independent of an air gap.

ACKNOWLEDGMENT

Authors acknowledge the support provided by Manipal Institute of Technology, Manipal Academy of Higher Education, Manipal and ME Department of National Institute of Technology Karnataka, Surathkal for carrying out the research work.

REFERENCES

1. Backers, F. T., "A magnetic journal bearing," *Philips Tech. Rev.*, Vol. 22, 232–238, 1960–61.
2. Yonnet, J. P., "Passive magnetic bearings with permanent magnets," *IEEE Trans. Magn.*, Vol. 14, No. 5, 803–805, 1978.
3. Yonnet, J. P., "Permanent magnetic bearings and couplings," *IEEE Trans. Magn.*, Vol. 17, No. 1, 1169–1173, 1981.
4. Schweitzer, G., "Magnetic bearings-applications, concepts and theory," *JSME International Journal, Series III*, Vol. 3, 13–18, 1990.
5. Fang, J., Y. Le, J. Sun, and K. Wang, "Analysis and design of passive magnetic bearing and damping system for high-speed compressor," *IEEE Trans. Magn.*, Vol. 48, No. 9, 2528–2537, 2012.
6. Morales, W., R. Fusaro, and A. Kascak, "Permanent magnetic bearing for spacecraft applications," *Tribology Transactions*, Vol. 46, No. 3, 460–464, 2003.
7. Bekinal, S. I., S. Jana, and S. S. Kulkarni, "A hybrid (permanent magnet and foil) bearing set for complete passive levitation of high-speed rotors," *Proc. IMechE, Part C: J. Mechanical Engineering Science*, Vol. 231, 3679–3689, 2017.
8. Sotelo, G. G., R. Andrade, and A. C. Ferreira, "Magnetic bearing sets for a flywheel system," *IEEE Trans. on Applied Super Conductivity*, Vol. 17, No. 2, 2150–2153, 2007.
9. Marinescu, M. and N. Marinescu, "A new improved method of for computation of radial stiffness of permanent magnet bearings," *IEEE Trans. Magn.*, Vol. 30, 3491–3494, 1994.
10. Delamare, J., E. Rulliere, and J. P. Yonnet, "Classification and synthesis of permanent magnet bearing configurations," *IEEE Trans. Magn.*, Vol. 31, No. 6, 4190–4192, 1995.
11. Lang, M., "Fast calculation method for the forces and stiffness of permanent-magnet bearings," *Proceedings of Eighth International Symposium on Magnetic Bearings*, 533–537, Mito, Japan, 2002.
12. Jiang, S., Y. Liang, and H. Wang, "A simplified method of calculating axial force for a permanent magnetic bearing," *Proc. IMechE, Part C: J. Mechanical Engineering Science*, Vol. 224, 703–708, 2009.
13. Samanta, P. and H. Hirani, "Magnetic bearing configurations: Theoretical and experimental studies," *IEEE Trans. Magn.*, Vol. 44, No. 2, 292–300, 2008.
14. Ravaut, R., G. Lemarquand, and V. Lemarquand, "Force and stiffness of passive magnetic bearings using permanent magnets. Part 1: Axial magnetization," *IEEE Trans. Magn.*, Vol. 45, No. 7, 2996–3002, 2009.
15. Ravaut, R., G. Lemarquand, and V. Lemarquand, "Force and stiffness of passive magnetic bearings using permanent magnets. Part 2: Radial magnetization," *IEEE Trans. Magn.*, Vol. 45, No. 9, 3334–3342, 2009.
16. Bekinal, S. I., T. R. Anil, and S. Jana, "Analysis of axially magnetized permanent magnet bearing characteristics," *Progress In Electromagnetics Research B*, Vol. 44, 327–343, 2012.
17. Bekinal, S. I., T. R. Anil, and S. Jana, "Analysis of radial magnetized permanent magnet bearing characteristics for five degrees of freedom," *Progress In Electromagnetics Research B*, Vol. 52, 307–326, 2013.
18. Bekinal, S. I., T. R. Anil, S. Jana, S. S. Kulkarni, A. Sawant, N. Patil, and S. Dhond, "Permanent magnet thrust bearing: Theoretical and experimental results," *Progress In Electromagnetics Research B*, Vol. 56, 269–287, 2013.
19. Yonnet, J. P., G. Lemarquand, S. Hemmerlin, and E. Olivier-Rulliere, "Stacked structures of passive magnetic bearings," *Journal Applied Physics*, Vol. 70, 6633–6635, 1991.

20. Paden, B., N. Groom, and J. Antaki, "Design formulas for permanent-magnet bearings," *ASME Trans.*, Vol. 125, 734–739, 2003.
21. Tian, L.-L., X.-P. Ai, and Y.-Q. Tian, "Analytical model of magnetic force for axial stack permanent-magnet bearings," *IEEE Trans. Magn.*, Vol. 48, No. 10, 2592–2599, 2012.
22. Bekinal, S. I. and S. Jana, "Generalized three-dimensional mathematical models for force and stiffness in axially, radially, and perpendicularly magnetized passive magnetic bearings with 'n' number of ring pairs," *ASME Journal of Tribology*, Vol. 138, No. 3, 031105(1–9), 2016.
23. Moser, R., J. Sandtner, and H. Bleuler, "Optimization of repulsive passive magnetic bearings," *IEEE Trans. Magn.*, Vol. 42, No. 8, 2038–2042, 2006.
24. Lijesh, K. P., M. R. Doddamani, and S. I. Bekinal, "A pragmatic optimization of axial stack-radial passive magnetic bearings," *ASME Journal of Tribology*, Vol. 140, 021901(1–9), 2018.
25. Bekinal, S. I., M. R. Doddamani, and N. D. Dravid, "Utilization of low computational cost two dimensional analytical equations in optimization of multi rings permanent magnet thrust bearings," *Progress In Electromagnetics Research M*, Vol. 62, 51–63, 2017.
26. Beneden, M. V., V. Kluyskens, and B. Dehez, "Optimal sizing and comparison of permanent magnet thrust bearings," *IEEE Trans. Magn.*, Vol. 53, No. 2, 2017.
27. Bekinal, S. I., M. R. Doddamani, and S. Jana, "Optimization of axially magnetised stack structured permanent magnet thrust bearing using three dimensional mathematical model," *ASME Journal of Tribology*, Vol. 139, No. 3, 031101(1–9), 2017.
28. Bekinal, S. I., M. R. Doddamani, B. V. Mohan, and S. Jana, "Generalized optimization procedure for rotational magnetized direction permanent magnet thrust bearing configuration," *Proc. IMechE, Part C: J. Mechanical Engineering Science*, Vol. 233, 2563–2573, 2019.
29. Lijesh, K. P., M. R. Doddamani, S. I. Bekinal, and S. M. Muzakkir, "Multi-objective optimization of stacked radial passive magnetic bearing," *Proc. IMechE Part J: J. Engineering Tribology*, Vol. 232, 1140–1159, 2018.
30. Filatov, A., L. Hawkins, V. Krishnan, and B. Lam, "Active axial electromagnetic damper," *Proceedings of Eleventh International Symposium on Magnetic Bearings*, 2000.
31. Cheah, S. K. and H. A. Sodano, "Novel eddy current damping mechanism for passive magnetic bearings," *Journal of Vibration and Control*, Vol. 14, No. 11, 1749–1766, 2008.
32. Yoo, S. Y., W. Kim, S. Kim, W. Lee, Y. Bae, and M. Noh, "Optimal design of non-contact thrust bearing using permanent magnet rings," *Int. Journal of Precision Engg. and Manufacturing*, Vol. 12, No. 6, 1009–1014, 2011.
33. Safaeian, R. and H. Heydari, "Comprehensive comparison of different structures of passive permanent magnet bearings," *IET Electric Power Appl.*, Vol. 12, 179–187, 2017.